FIFTH INTERNATIONAL CONGRESS ON SOUND AND VIBRATION

DECEMBER 15-18, 1997
ADELAIDE, SOUTH AUSTRALIA

Invited Paper

COMPARATIVE STUDY OF BOUNDARY ELEMENT AND FINITE ELEMENT FORMULATIONS FOR EVALUATING SOUND RADIATION FROM PLATES

Jean-Pierre Coyette and Luc Cremers

LMS-Numerical Technologies
Leuven, Belgium

ABSTRACT

The present paper deals with a practical comparison of BE and FE methods as they could be applied to sound radiation from a baffled elastic plate subjected to a point load. Such an application is representative of a wider class of vibro-acoustic problems where a time-harmonic mechanical excitation is driving a structure which in turns radiates sound in the surrounding fluid. The numerical treatment of this problem is performed by combining a structural FE model (and his related modal representation) with an acoustic FE or BE model.

1. INTRODUCTION

Modeling sound radiation from vibrating structures usually relies, at least in the 'low' frequency range, on boundary integral representations of the acoustic field. Either direct and indirect integral representations are available for that purpose and form the mathematical basis of related acoustic boundary element (BE) methods [Ciskowski and Brebbia, 1991]. Such formulations have been used for a long time by the acoustic community. Model size's reduction and *a priori* verification of the Sommerfeld radiation condition are presented as key characteristics of BE methods. On the other hand, domain methods (like finite element (FE) methods) require an appropriate treatment of the radiation condition, involve usually a larger amount of data (as implied by the related volume mesh) but are characterized by sparse matrices and reduced calculation times.

The acoustic FE model relies on variable order infinite wave envelope elements [Astley, Macaulay and Coyette, 1994; Cremers, Fyfe and Coyette, 1994] for handling approximately the Sommerfeld radiation condition. Different classes of infinite wave envelope elements (spherical and spheroidal) of variable order [SYSNOISE, 1996] have been used for that purpose. A comparison of results associated to different models is presented for this particular benchmark problem. Both field values (acoustic pressures) and integrated values (radiated power) are involved in this comparison. They show the capability of infinite element formulations to resolve the acoustic field in the vicinity of a vibrating structure.

2. BENCHMARK DEFINITION

The problem considered is related to sound radiation from an baffled elastic plate (Figure 1) excited by a point load. This problem is extracted from a set of benchmarks published by SFM (Société Française de Mécanique) as a first guide for validating vibro-acoustic softwares [Valor, 1996].

The following data are used for the elastic plate (length a = 1 m, length b = 1 m, thickness t = 0.01 m, Young modulus $E = 2.10^{+11}$ Pa, Poisson ratio $\nu = 0.3$, density $\rho = 7800$ kg/m^3, structural loss factor $\eta = 10^{-2}$). The plate is simply supported along the four edges and is surrounded by a rigid (plane) baffle. The acoustic fluid (on one side of the plate) is the air with conventional material properties (density $\rho = 1.2$ kg/m^3 and speed of sound c = 340 m/s). A point load of amplitude F = 1 N (with a time dependence like $e^{+i\omega t}$ where ω is the circular frequency) is applied at location ($x_1 = 0.2$ m, $x_2 = -0.3$ m).

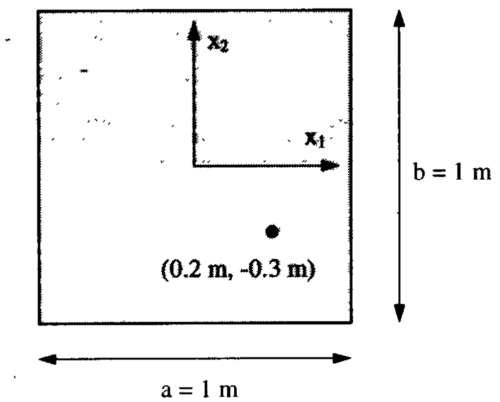

Figure 1: Elastic plate problem.

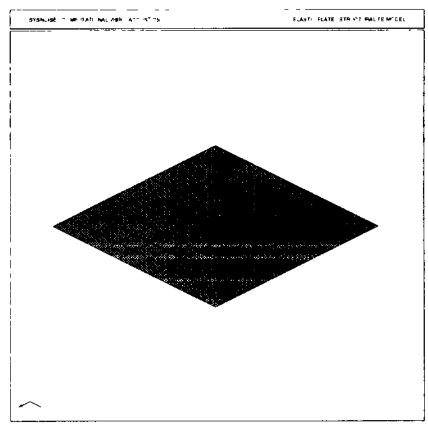

Figure 2: Elastic plate - FE mesh (100 QUAD4, 121 nodes).

3. NUMERICAL MODELS

The problem has been modeled using two particular coupled methods. Both methods refer to a conventional structural FE model for the plate. The first method combines this structural FE model with an acoustic BE model (based on Rayleigh's integral representation for baffled problems) while the second one combines the structural FE model with an acoustic FE model where the 'far' field is modeled by infinite wave envelope elements [Astley, Macaulay and Coyette, 1994]. The coupled effects are taken into account in the usual way [Morand and Ohayon, 1995] so that the discrete coupled system can be formulated as:

$$\begin{bmatrix} Z_S(\omega) & C \\ \rho\omega^2 C^T & Z_A(\omega) \end{bmatrix} \begin{pmatrix} U \\ P \end{pmatrix} = \begin{pmatrix} F_S \\ F_A \end{pmatrix} \tag{1}$$

where Z_S and Z_A are the structural and acoustic impedance matrices, C is the geometrical coupling matrix, F_S and F_A are the structural and acoustical load vectors, U and P are the vectors of nodal displacements (or modal participation factors) and nodal pressures. Details are omitted here but can be found in references listed at the end of the paper.

3.1 Structural FE model

The FE structural mesh is represented in Figure 2 (100 QUAD4 thin shell elements). A reduced modal basis involving the first 25 eigenmodes has been selected. The related eigenfrequencies and modal orders along x_1- and x_2-directions are listed in Table 1.

Mode	Hz	Mode	Hz	Mode	Hz	Mode	Hz	Mode	Hz
(1,1)	48.140	(2,1)	120.35	(3,1)	240.70	(4,1)	409.19	(5,1)	625.82
(1,2)	120.35	(2,2)	192.56	(3,2)	312.91	(4,2)	481.40	(5,2)	698.03
(1,3)	240.07	(2,3)	312.91	(3,3)	433.26	(4,3)	601.75	(5,3)	818.38
(1,4)	409.19	(2,4)	481.40	(3,4)	601.75	(4,4)	770.24	(5,4)	986.87
(1,5)	625.82	(2,5)	698.03	(3,5)	818.38	(4,5)	986.87	(5,5)	1203.5

Table 1: Elastic plate - First 25 eigenfrequencies.

3.2 Acoustic BE model

The acoustic BE model relies on Rayleigh's integral representation (as valid for a baffled plane structure). The related BE mesh is identical to the structural FE mesh shown in Figure 2. This acoustic BE model (coupled to the above structural FE model) produces a solution nearly identical (at least in the considered frequency range) to the available reference solution [Valor, 1996].

3.3 Acoustic FE models

Various acoustic FE models have been used for this benchmark. All these models rely on a conventional pressure formulation for the acoustic fluid and a suitable volume mesh in the vicinity of the vibrating structure. This particular 'inner' domain correspond to either a box (Figure 3) for meshes A1 and A2 (Figure 5) or a semi-ellipsoid (Figure 4) for meshes A3 and A4 (Figure 6).

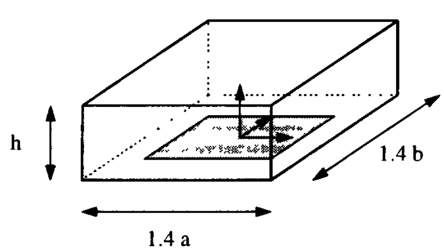

Figure 3: 'Inner' acoustic domain related to meshes A1 (h=0.5 a) and A2 (h=0.3 a).

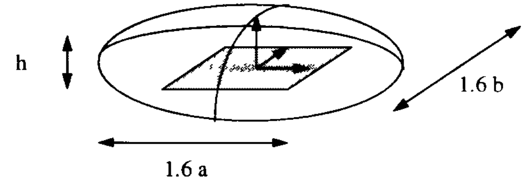

Figure 4: 'Inner' acoustic domain related to meshes A3 (h=0.25 a) and A4 (h=0.10 a).

The models differ by the nature of infinite wave envelope elements selected for the 'outer' field. 'Spherical' infinite elements are used in conjunction with meshes A1 and A2 while 'oblate spheroidal' infinite elements are selected for meshes A3 and A4. It should be emphasized that meshes A1 and A2 violate the 'circumscribing' sphere condition while the external ellipsoidal boundary surface of meshes A3 and A4 is enclosing totally the vibrating structure.

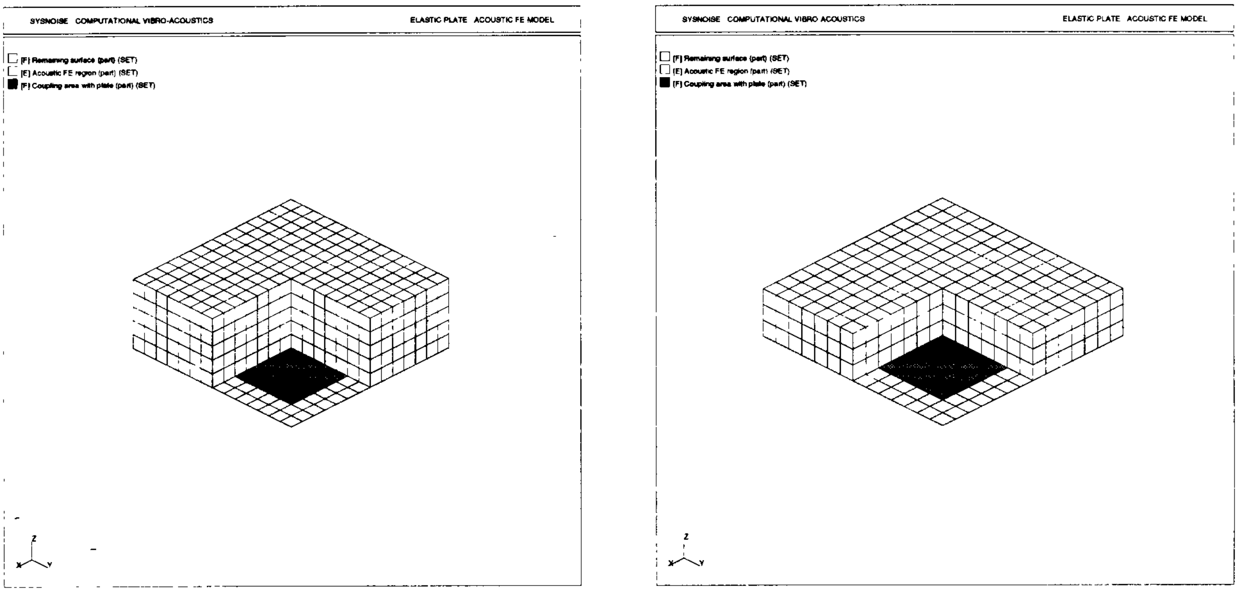

Figure 5: Acoustic FE meshes A1 (left; 1350 nodes and 980 elements) and A2 (right; 900 nodes and 588 elements).

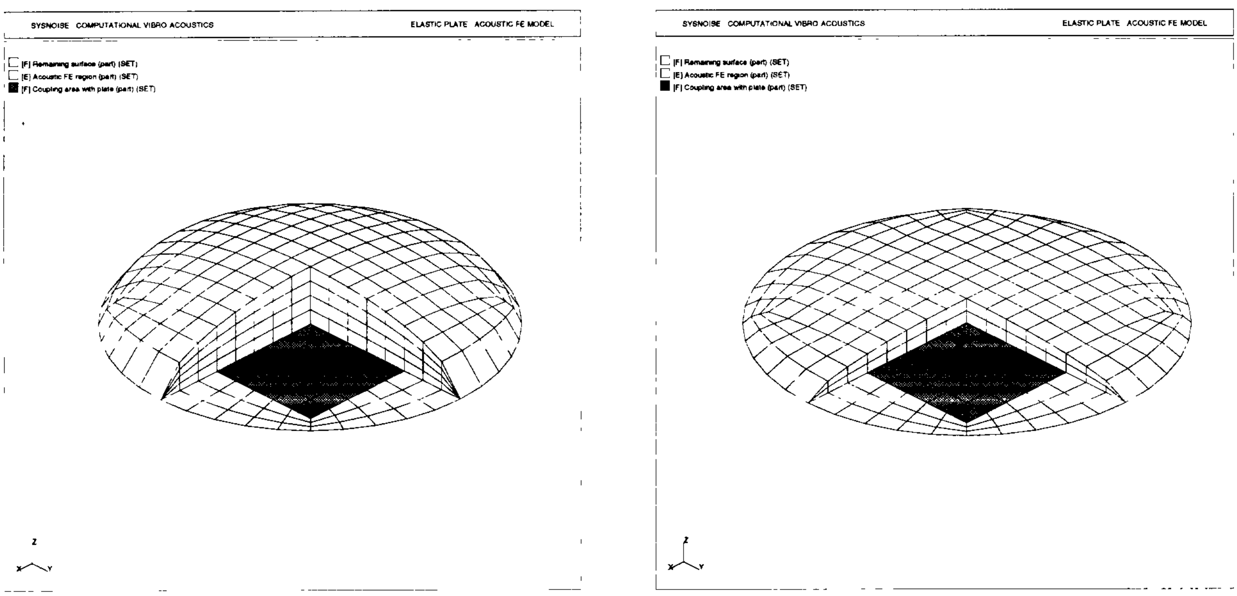

Figure 6: Acoustic FE meshes A3 (left; 1045 nodes and 880 elements) and A4 (right; 643 nodes and 440 elements).

4. NUMERICAL RESULTS

The acoustic response has been evaluated for the different models in the frequency range 10-300 Hz using a step of 1 Hz. For each model, attention has been paid to single field values (pressure at two field points located at (P1: $x_1=0$, $x_2=0$, $x_3=0$) and at (P2: $x_1=0$, $x_2=0$, $x_3=1$) but also to integrated quantities. For the acoustic engineer, the radiated power W_{rad} is such a meaningful integrated quantity that can be evaluated from:

$$W_{rad}(\omega) = \int_S \mathrm{Re}\left(p(\mathbf{x},\omega)v_n^*(\mathbf{x},\omega)\right) dS(\mathbf{x}) \tag{2}$$

where p and v_n are the pressure and the normal velocity along the radiating surface S.

4.1 Spherical infinite elements

Field pressures at points P1 and P2 as obtained using mesh A1 and spherical infinite elements of order 1, 2 and 3 are presented in Figure 7. Similar results obtained with mesh A2 are presented in Figure 8. The radiated power as obtained using meshes A1 and A2 is presented in Figure 9.

The results obtained show an excellent agreement with the reference solution for elements of order greater or equal to 2 along the radial direction.

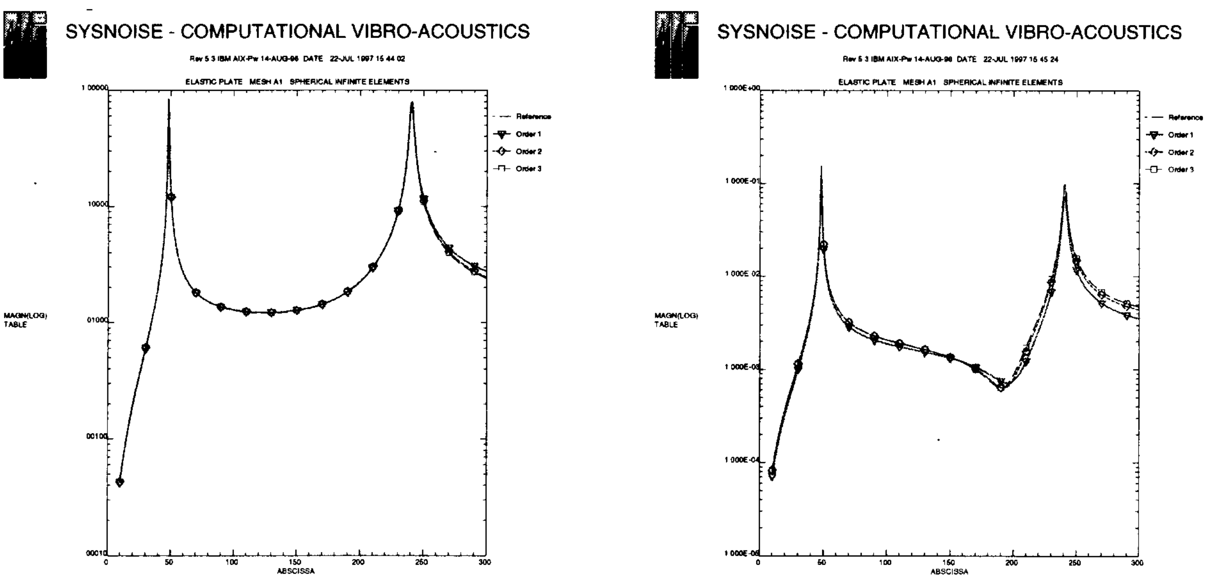

Figure 7: Magnitude of field pressure (log scale) at points P1 (left) and P2 (right) using mesh A1 (*spherical* infinite elements of order 1,2 and 3) compared to reference solution (SFM, 1996).

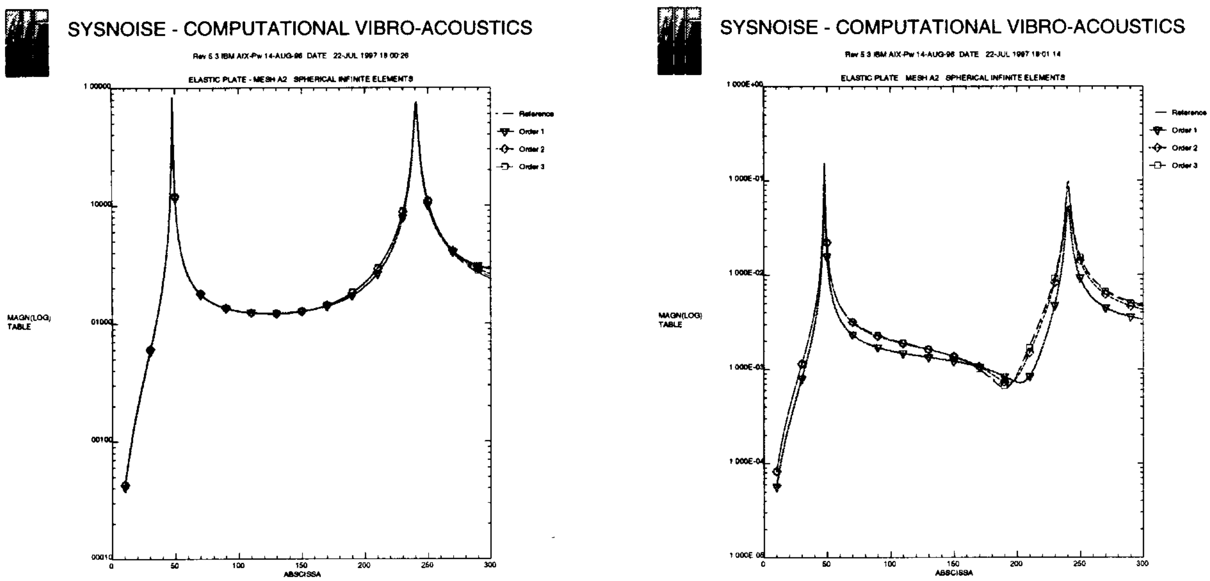

Figure 8: Magnitude of field pressure (log scale) at points P1 (left) and P2 (right) using mesh A2 (*spherical* infinite elements of order 1,2 and 3) compared to reference solution (SFM, 1996).

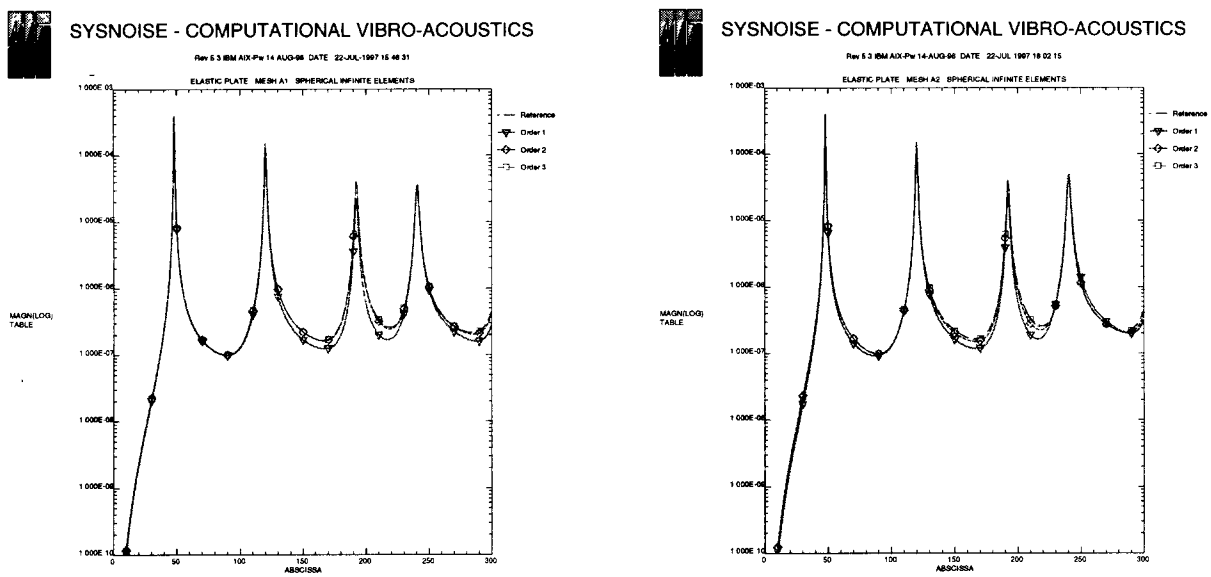

Figure 9: Radiated power (log scale) using mesh A1 (left) and A2 (right) (*spherical* infinite elements of order 1,2 and 3) compared to reference solution (SFM, 1996).

4.2 Oblate spheroidal infinite elements

In the same way, field pressures at points P1 and P2 as obtained using mesh A3 and oblate spheroidal infinite elements of order 1, 2 and 3 are presented in Figure 10. Similar results obtained with mesh A4 are presented in Figure 11. The radiated power as obtained using meshes A3 and A4 is presented in Figure 12.

As it can be seen from inspection of Figures 10 and 11, the convergence is still good along the radiating surface but deteriorates at greater distance.

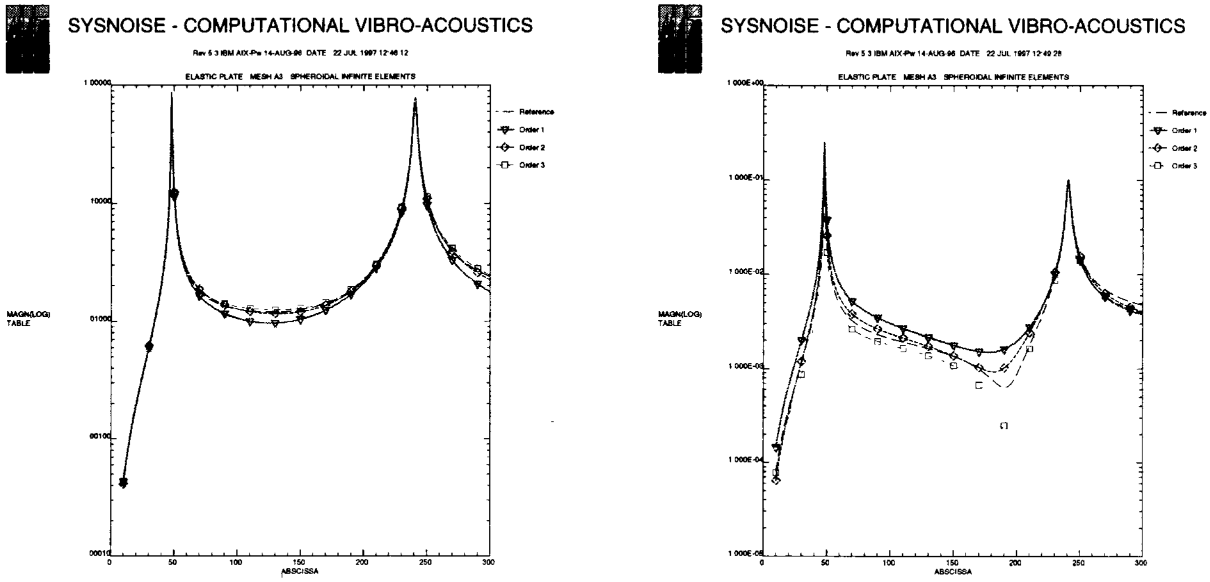

Figure 10: Magnitude of field pressure (log scale) at points P1 (left) and P2 (right) using mesh A3 (*oblate spheroidal* infinite elements of order 1,2 and 3) compared to reference solution (SFM, 1996).

5. CONCLUSION

A practical comparison of FE and BE results for a simple radiation problem involving a mechanically excited plate has been presented. The problem is representative of a wider class of problems arising in industrial applications. The combined use of finite and infinite elements allows to capture the reference solution available for that problem at least in the vicinity of the radiating structure as it can be seen from single value (field pressure at plate's center) and integrated value (radiated power) predictions. These good performances have been obtained for both spherical and oblate spheroidal infinite elements. On the other hand, spheroidal elements are leading (at least for the considered case) to a slower convergence that should be investigated in more details.

6. REFERENCES

Astley, R.J., Macaulay, G.J. and Coyette, J.P., 1994, "Mapped wave envelope elements for acoustical radiation and scattering", *Journal of Sound and Vibration*, Vol. 170, pp. 97-118.

Cremers, L., Fyfe, K.R. and Coyette, J.P., 1994, "A variable order infinite acoustic wave envelope element", *Journal of Sound and Vibration*, Vol. 171, pp. 483-508.

Burnett, D.S., 1994, "A three-dimensional acoustic infinite element based on prolate spheroidal multipole expansion", *J. Acoust. Soc. America*, Vol. 96, pp. 2789-2816.

Ciskowski, R.D. and Brebbia, C.A., 1991, *Boundary element methods in acoustics*, Computational Mechanics Publications, Boston.

Morand, H.J.P. and Ohayon, R., 1995, *Fluid-structure interaction*, John Wiley & Sons, Chichester.

SYSNOISE Revision 5.3, 1996, User's Manual, LMS-Numerical Technologies, Leuven (Belgium).
Valor, C., 1996, *Résultats de référence pour le rayonnement acoustique de plaques*, Société Française de Mécanique (SFM) - Société Française d'Acoustique (SFA), Commission de Validation des Progiciels de Calcul Vibroacoustique, ISBN 2-904983-11-2 (Published by SFM, Maison de la Mécanique, 39-41 rue Louis Blanc, 92400 Courbevoie, France).

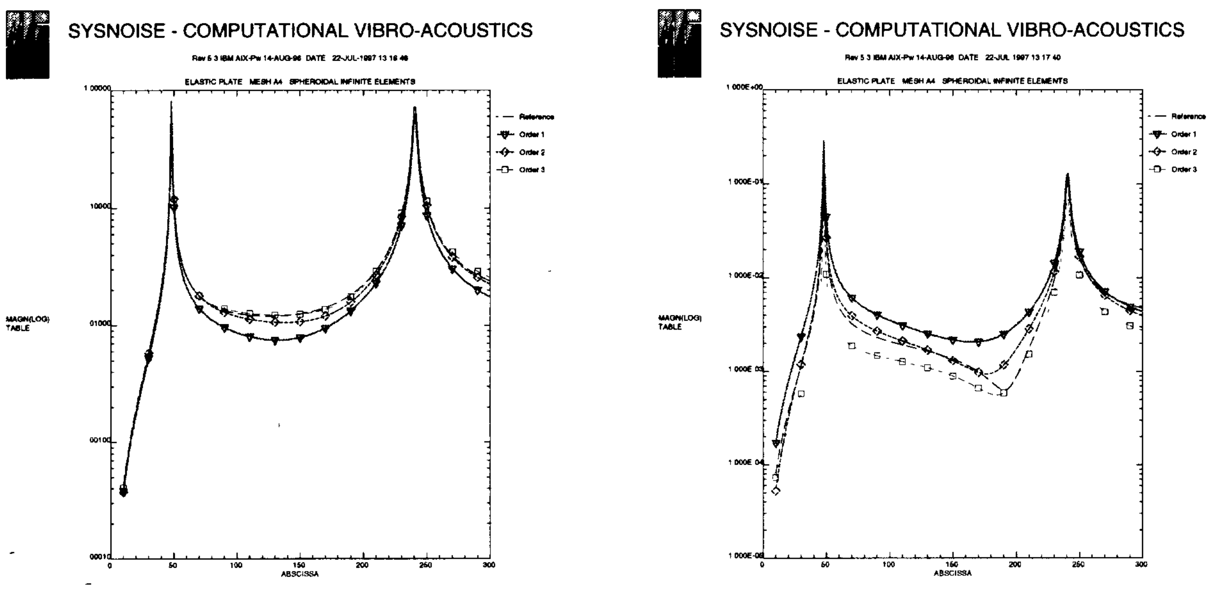

Figure 11: Magnitude of field pressure (log scale) at points P1 (left) and P2 (right) using mesh A4 (*oblate spheroidal* infinite elements of order 1,2 and 3) compared to reference solution (SFM, 1996).

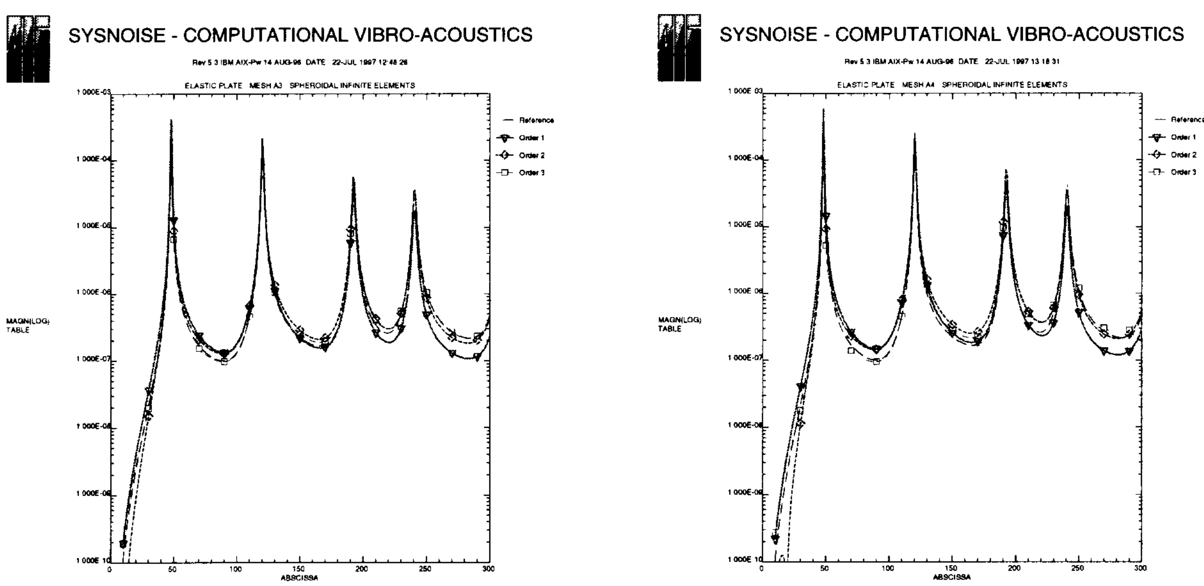

Figure 12: Radiated power (log scale) using mesh A3 (left) and A4 (right) (*oblate spheroidal* infinite elements of order 1,2 and 3) compared to reference solution (SFM, 1996).